ResearchGate

See discussions, stats, and author profiles for this publication at: https://www.researchgate.net/publication/234850559

Tunneling transport in polyoxometalate based composite materials

ARTICLE *in* APPLIED PHYSICS LETTERS · JULY 2003

Impact Factor: 3.3 · DOI: 10.1063/1.1594278

CITATIONS
34

READS
33

4 AUTHORS, INCLUDING:

N. Glezos
National Center for Scientific Research Demo…
76 PUBLICATIONS **676** CITATIONS
SEE PROFILE

Panagiotis Argitis
National Center for Scientific Research Demo…
192 PUBLICATIONS **1,898** CITATIONS
SEE PROFILE

D. Velessiotis
National Center for Scientific Research Demo…
20 PUBLICATIONS **177** CITATIONS
SEE PROFILE

Available from: Panagiotis Argitis
Retrieved on: 16 January 2016

Tunneling transport in polyoxometalate based composite materials

N. Glezos,[a] P. Argitis, D. Velessiotis, and C. D. Diakoumakos
Institute of Microelectronics, NCSR "Demokritos," 15310, Aghia Paraskevi, Greece

(Received 12 March 2003; accepted 21 May 2003)

Molecular materials containing tungsten polyoxometalates as the active elements embedded into polymer matrices are investigated as candidates for electronic device applications. The transport properties of these materials are investigated varying the interelectrode spacing and the polyoxometalate concentration. The $I-V$ characteristics of planar devices reveal a conductivity peak at room temperature conditions for intermolecular distances less than 3 nm and electrode distances less than 100 nm. The transport characteristics are discussed in terms of tunneling mechanisms. © *2003 American Institute of Physics.* [DOI: 10.1063/1.1594278]

Several molecular or nanocrystalline materials are currently being investigated as alternatives for present day microelectronics with the hope to reduce critical device dimensions to a few atom scale. Such materials include silicon nanowires and nanoclusters, metallic clusters, carbon nanotubes or fullerenes, and other organic molecules. Recently our group started a research effort for the investigation of possibilities for device applications offered by molecular systems having strong structural similarities to extended lattice semiconductors. In this context we investigate a class of molecular materials based on inorganic polyoxometalates.

Polyoxometalates (POMs) are a class of inorganic compounds that can be envisioned as soluble molecular semiconducting oxides.[1–3] These compounds for reasons of cationic radius size and oxygen $p\pi$ bonding capabilities can be formed having as basis only five elements of the periodic table (V, Nb, Ta, Mo, W) but the most stable and well characterized elements that offer substantial chemical handling capability and property tunability are W and Mo. The tungsten and molybdenum POMs are known for their well defined and stable structure as well as for their reduction oxidation (redox) thermal or photochemical reactions and catalytic properties.[4] These compounds have been already characterized as zero-dimension semiconductors from their behavior in catalytic applications. Metal[5–7] and silicon[8] nanoclusters have been used in single electron transistors or hybrid devices based on Coulomb blockade effects. In these devices room temperature operation requires clusters of about 1 nm.[9] Polyoxometalates do not suffer from the limitations of size and process reproducibility. They are stable oxides with fixed dimensions ~1 nm. Their charging energies are in the range 0.1–4.0 eV, much higher than those of metallic nanoclusters therefore the resolution of discrete electronic levels at room temperature conditions is expected. The earlier characteristics makes them attractive for applications where charge confinement is required, e.g., as a control gate element in a hybrid molecular-silicon flash memory device.

In this letter we describe the formulation of composite materials consisting of tungsten polyoxometalates embedded in polymeric matrices and we investigate the conductivity mechanisms in the nanometer region. The well known Keggin structure polyoxomatalate $(PW_{12}O_{40})^{3-}$ is used in this study embedded in acid form in poly(methylmethacrylate) (PMMA) matrix. Other polymeric materials have also been tested as matrices.[10,11] A suitable host material should not react with the embedded molecules, thus altering their transport properties, and at the same time the composite material should preferably behave as a lithographic resist with nanometer resolution for nanofabriation process simplification reasons. On the other hand the molecular structure and concentration of the guest material should remain unchanged throughout the lithographic process. PMMA based formulations meet the earlier demands in a satisfactory manner. Electron beam exposure and development processing have no effect on the tungsten POM structure and concentration as manifested by monitoring possible changes through its characteristic UV absorption spectrum during processing.

Solutions of $H_3(PW_{12}O_{40})$ and high molecular weight PMMA into PGMEA solvent were prepared. The relative weight concentration POM/PMMA was varied in the range 1:4 w/w up to 5:1 w/w in order to examine the dependence of the transport characteristics upon the mean distance of the active molecules. By 1:1 w/w we mean equal weights of POM and PMMA. The 1:4 formulation corresponds to a mean molecular distance of approximately $\langle d\rangle = 2.8$ nm in solid film. Given that the size of the POM molecules is approximately 1 nm the approaching distance for electron hopping between molecules is $\langle d\rangle = 1.6$ nm. Under the same conditions the corresponding value for a 5:1 concentration is $\langle d\rangle = 0.5$ nm.

Next, the lithographic properties of the POM/PMMA composites were tested. Films of 300 nm for electron (e)-beam lithography were prepared by spinning at 4000 rpm for 30 s and prebaking at 160 °C for 1 h. Development was done in methylisobutylketone–isopropyl alcohol 1:3 for 30 s. The absorption spectrum was examined between the processing steps in order to ensure that the POM concentration remains unchanged.[11] We proved that the e-beam lithography resolution properties and etch resistance properties of PMMA are enhanced due to the presence of POM. The dose required is 30% higher since a part of the incident energy is absorbed by the POMs thus not contributing to chain scission. These re-

[a]Electronic mail: glezos@imel.demokritos.gr

 © 2003 American Institute of Physics
Downloaded 28 Jun 2004 to 143.233.248.110. Redistribution subject to AIP license or copyright, see http://apl.aip.org/apl/copyright.jsp

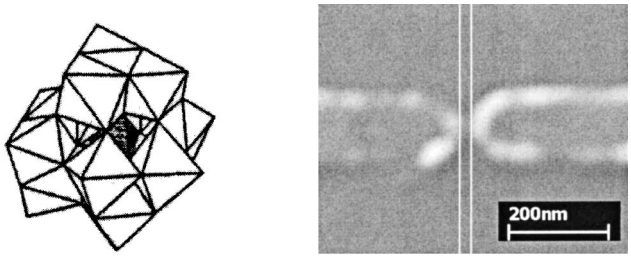

FIG. 1. (a) Keggin structure of the $(PW_{12}O_{40})^{3-}$ tungsten polyoxometalates used in this paper. The P hetero atom occupies the center of the structure while the W atoms are at the centers of the regular polyedra with oxygen atoms at the vertices. (b) A PMMA lift-off process was used for the definition of electrodes with minimum distance 10 nm.

sults have been checked experimentally as well as by electron beam exposure simulation methods.[12,13]

We investigated the dependence of the conducting behavior upon the electrode distance. Aluminum electrodes were patterned on a SiO_2 surface using electron beam lithography (50 keV, EBPG-3, Leica) and a lift-off process in an ultrasonic bath. Interelectrode distances of 10 nm up to 40 μm were defined on the same sample to enable the comparison of conductivity curves (Fig. 1). The structure of the $I-V$ characteristic depends upon the intermolecular distance and the electrode spacing. Tunneling effects expressed as conductivity peaks appear when the intermolecular distance $\langle d \rangle$ less than 3 nm (corresponding to a POM/PMMA relative concentration of 1:1 w/w) and the electrode spacing is less than 100 nm. In the case of higher POM concentrations the current follows a space charge limited (SCL) square law $I-V^2$ or even a linear Ohmic law. The situation is typical for one type of carriers in the presence of traps, in this case the tungstate molecules. Electrical measurements were unstable in the case of smaller tungstate concentrations (e.g., in the 1:4 case) due to large fluctuations of the number of the active molecules in the conductive channel. The dependence of tunneling effects upon electrode distance is shown in Fig. 2. In

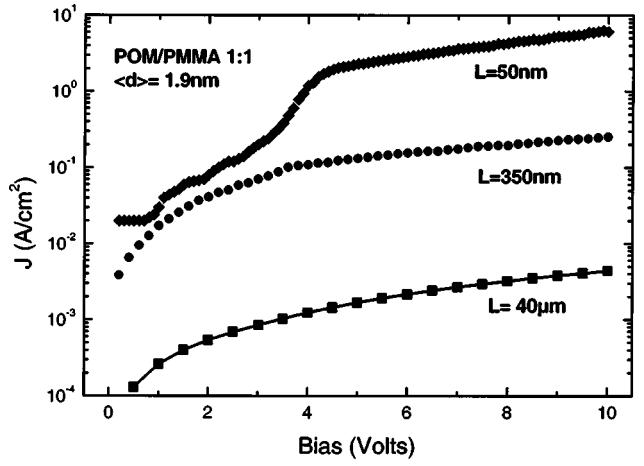

FIG. 2. $I-V$ in the case of a POM/PMMA 1:1 w/w material with aluminum electrodes distant $L=40$ μm (■), 350 nm (●), and 50 nm (♦) apart. In the 40 μm case the solid line is the SCL law. For smaller electrode distances a conductivity peak appears at 3.5 V.

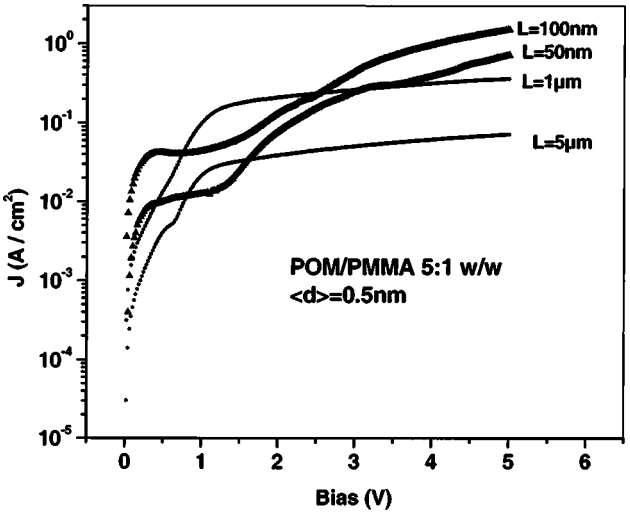

FIG. 3. $I-V$ for a POM/PMMA 5:1 w/w material. In the case of electrode distances in the submicrometer region (large symbols), a plateau appears due to tunneling effects.

the case of larger electrode distances the current follows a SCL law of the form

$$J=\frac{9}{8}\epsilon_s \mu \frac{V^2}{d^3}, \tag{1}$$

where ϵ_s is the dielectric constant, d is the intermolecular distance, and μ is the carrier mobility. Mobility is limited by the hoping mechanism between molecules. The value calculated using Eq. (1) in the case of the POM/PMMA 1:1 w/w material presented in Fig. 2 is 4×10^{-5} $cm^2/V\,s$. This value increases when electrodes are approaching since the conductivity paths become better defined in small geometries. The largest value measured is 4×10^{-3} $cm^2/V\,s$ in the 25 nm case. Tunneling effects become evident for $L<350$ nm in the 1:1 case where a conductivity peak around 3.5 V appears. This peak is more pronounced in the case of smaller distances. For voltage values greater than this threshold a SCL square law is still valid. The dependence of the $I-V$ characteristics upon the electrode distance was also examined for higher POM concentrations as for example in Fig. 3 for a POM/PMMA 5:1 w/w material. The transport behavior is slightly different. In the case of higher electrode distances ($L=1$ and 5 μm in Fig. 3) the $I-V$ follows an ohmic law while in the case of smaller distances $L<100$ nm there is a plateau region and a conductivity peak in the range 1–2 V lower than the corresponding value for the 1:1 case. This is due to the lower tunneling distance and the higher charge concentration.

In the case of nanometer distant aluminum electrodes the $I-V$ characteristic may be divided into three parts: (a) the low voltage region, (b) the region around the conductivity peak, and (c) the SCL region. In the case of low bias voltages tunneling mechanisms dominate transport. A detailed theoretical model in this case should take into account both tunneling through the aluminum oxide barriers as well as multiple tunneling between the molecules.[14] However a simple tunneling model through a metal–insulator–metal (MIM) structure provides a good fit of the experimental results. Simmons[15] derived an analytical solution for the electron

Downloaded 28 Jun 2004 to 143.233.248.110. Redistribution subject to AIP license or copyright, see http://apl.aip.org/apl/copyright.jsp

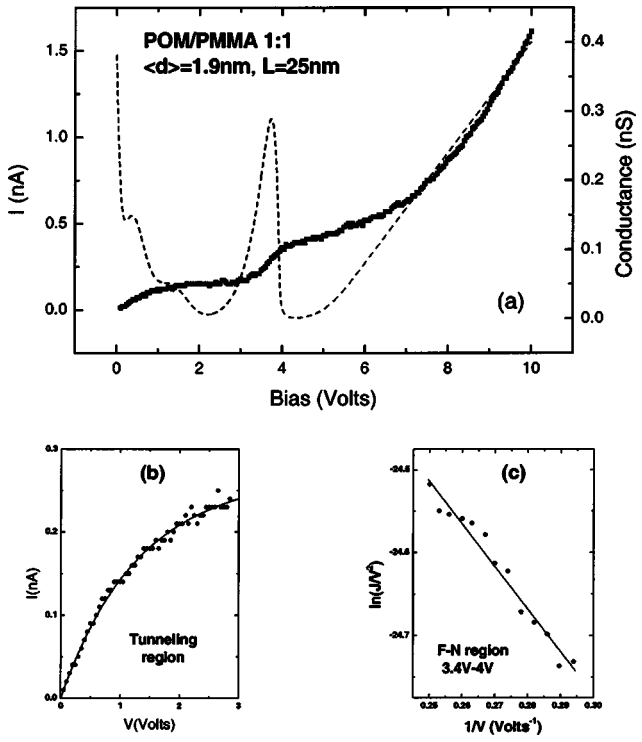

FIG. 4. (a) Current (solid line) and conductance (dashed line) curves in the case of a 1:2 POM/PMMA composite with electrode distance $L=25$ nm. The intermolecular distance of POMs is estimated to be 1.9 nm in this concentration. Given that the molecular size is approximately 1 nm, the average electron path in the case of the 50 nm electrodes consists of 8–10 tunneling events. The low voltage plateau (b) is discussed in terms of low voltage tunneling and the region of the conductivity peak in terms of the Fowler–Nordheim mechanism (c). For larger values a SCL law is valid leading to a linear conductance.

current through a MIM structure with a thin insulating barrier of length d. The expression derived by Simmons and used in the present work is

$$I=I_0[\Phi\cdot\exp(-\alpha\sqrt{\Phi})-(\Phi+\mathrm{eV})\cdot\exp(-\alpha\sqrt{\Phi+\mathrm{eV}})], \tag{2}$$

where $\alpha=2d\sqrt{2m}/\hbar$ and Φ is the mean barrier height for the whole system

$$\Phi=\frac{\Phi_{\mathrm{ox}}d_{\mathrm{ox}}+\Phi_f d_f}{d_{\mathrm{ox}}+d_f}, \tag{3}$$

where Φ_{ox}, d_{ox} are the native oxide barrier height and thickness and Φ_f, d_f the corresponding values for the POM film. The intermediate region (3.4–4.2 V in Fig. 4) is discussed in terms of the Fowler–Nordheim (F–N) mechanism using a $\log(1/V^2)$ vs $1/V$ plot. Combining data from the two regions[16] the barrier height of the Al/POM contact may be evaluated. In the case of Fig. 4, $\Phi_f=0.20$ eV with $\Phi_{\mathrm{ox}}=4.2$ eV. Above the F–N region $V>4.2$ V the $I-V$ follows a SCL law. When the contact is illuminated the conductivity peak shifts to higher values, the current increases by one order of magnitude and the SCL region becomes linear. This is due to the addition of the photoelectrons through excitation from the highest occupied molecular orbital to the lowest unoccupied molecular orbital state of the molecule and eventually to hole transport. Such behavior has been previously reported for other molecular systems with nanometer contacts.[17] A more systematic study of the transport dependence upon the light wavelength is required in order to validate this assertion.

In summary, we investigated the transport characteristics of planar devices containing POM/PMMA composite materials as the active element. The $I-V$ curve was investigated with POM concentration and electrode distance as parameters. It was found that conductivity peaks appear at room temperature conditions for electrode distances smaller than 100 nm and a mean molecular separation smaller than 2–3 nm. Transport is discussed in terms of tunneling mechanisms. Preliminary work of the same group with vertical type structures has shown that the fabrication of resonant tunneling devices based on POMs is possible.[18] These properties, taking also into account the lithographic capability of the composites, make POMs promising for future molecular device applications.

[1] Chem. Rev. (Washington, D.C.) **98**, 1 (1998).
[2] M. T. Pope, *Heteropoly and Isopoly Oxometallates* (Springer, Berlin, 1983).
[3] M. T. Pope and A. Muller, Angew. Chem., Int. Ed. Engl. **30**, 34 (1991).
[4] A. Hiskia, A. Mylonas, and E. Papaconstantinou, Chem. Soc. Rev. **30**, 62 (2001).
[5] L. Clarke, M. N. Wybourne, M. Yan, S. X. Cai, and J. W. Keana, Appl. Phys. Lett. **71**, 617 (1997).
[6] A. Pepin, C. Vieu, H. Lanois, M. Rosmeulen, M. Van Rossum, H. O. Mueller, D. Williams, H. Mizuta, and K. Nakazato, Microelectron. Eng. **53**, 265 (2000).
[7] R. J. M. Vullers, M. Ahlskog, M. Cannaerts, and C. Van Haesendonck, Appl. Phys. Lett. **76**, 1947 (2000).
[8] Z. A. K. Durrani, A. C. Irvine, and H. Ahmed, Appl. Phys. Lett. **74**, 1293 (1999).
[9] E. Kapetanakis, P. Normand, and D. Tsoukalas, Appl. Phys. Lett. **80**, 2794 (2002).
[10] P. Argitis, R. A. Srinivas, J. C. Carls, and A. Heller, J. Electrochem. Soc. **139**, 2889 (1992).
[11] N. Glezos, P. Argitis, D. Velessiotis, P. Koutsolelos, C. D. Diakoumakos, A. Tserepi, and K. Beltsios, MRS 2001 Fall Meeting, paper Y2.5, online proceedings.
[12] N. Glezos and I. Raptis, IEEE Trans. Comput.-Aided Des. **15**, 92 (1996).
[13] X. Zianni, D. Velessiotis, N. Glezos, and K. N. Trohidou, Microelectron. Eng. **57–58**, 297 (2001).
[14] C. Kergueris, J. P. Bourgoin, S. Palacin, D. Esteve, C. Urbina, M. Magoga, and J. Joachim, Phys. Rev. B **59**, 12505 (1999).
[15] J. G. Simmons, J. Appl. Phys. **34**, 1793 (1963).
[16] Y. Isono and H. Nakano, J. Appl. Phys. **75**, 4557 (1994).
[17] R. Rinaldi, E. Branca, R. Cingolani, S. Masiero, G. P. Spada, and G. Gottarelli, Appl. Phys. Lett. **78**, 3541 (2001).
[18] N. Glezos, D. Velessiotis, G. Chaidogiannos, P. Argitis, D. Tsamakis, and X. Zianni, Synth. Met. **138**, 267 (2003).

Downloaded 28 Jun 2004 to 143.233.248.110. Redistribution subject to AIP license or copyright, see http://apl.aip.org/apl/copyright.jsp